

Effect of isovector scalar meson on equation of state of dense matter within relativistic mean field model

Virender Thakur,^{1,*} Raj Kumar,^{1,†} Pankaj Kumar,² Vikesh Kumar,¹
Mukul Kumar,¹ C. Mondal,³ B.K. Agrawal,^{4,‡} and Shashi K. Dhiman^{1,5,§}

¹*Department of Physics, Himachal Pradesh University, Shimla-171005, India*

²*Department of Applied Sciences, CGC College of Engineering, Landran, Mohali 140307, India*

³*Laboratoire de Physique Corpusculaire, CNRS, ENSICAEN, UMR6534,
Université de Caen Normandie, F-14000, Caen Cedex, France*

⁴*Saha Institute of Nuclear Physics, 1/AF Bidhannagar, Kolkata 700064, India*

⁵*School of Applied Sciences, Himachal Pradesh Technical University, Hamirpur-177001, India*

The effects of the isovector-scalar δ -meson field on the properties of finite nuclei, infinite nuclear matter and neutron stars are investigated within the Relativistic Mean Field (RMF) model which includes non-linear couplings. Several parameter sets (SRV's) are generated to assess the influence of δ -meson on the properties of neutron star. These parametrizations correspond to different values of coupling constant of δ -meson to the nucleons with remaining ones calibrated to yield finite nuclei and infinite nuclear matter properties consistent with the available experimental data. It is observed that to fit the properties of finite nuclei and infinite nuclear matter, a stronger coupling between isovector-vector ρ meson and nucleons is required in the presence of δ field. Furthermore, the δ -meson is found to affect the radius of canonical neutron star significantly. The value of dimensionless tidal deformability, Λ for the canonical neutron star also satisfies the constraints from the waveform models analysis of GW170817 binary neutron star merger event. A covariance analysis is performed to estimate the statistical uncertainties of the model parameters as well as correlations among the model parameters and different observables of interest.

I. INTRODUCTION

Neutron stars are the densest objects in the observable universe and deep knowledge of the Equation of State (EoS) of the dense matter in beta-equilibrium is thus required to understand their behavior. It has been shown that the dense matter EoS must be treated relativistically [1, 2]. For this reason, relativistic mean field (RMF) models have been widely used to obtain a realistic description of the properties of finite nuclei, bulk nuclear matter or the properties of neutron stars. Currently, many different variants of RMF models with various couplings are in use to study the finite nuclei and neutron star properties [3–5]. Accurate constraints are necessary to understand the limits of these different types of models. During the last decade, a wide range of astrophysical observations such as the precise measurement of massive millisecond pulsars using Shapiro delay technique [6, 7], detection of gravitational wave generated by binary neutron stars in the GW170817 event by the LIGO-Virgo collaboration [8, 9], or the joint mass radius measurement of neutron stars using X-ray timing technique by NICER collaboration [10–13] started to provide unprecedented new constraints on the dense matter EoS. They have triggered plethora of theoretical studies to look at the dense matter EoS from very different perspectives c.f. Ref. [14] and references therein. First of its kind model independent

measurement of neutron skin thickness Δr_{np} of ^{208}Pb [15] and ^{48}Ca [16] in the Jefferson lab also inspired theoretical studies to take a fresher look at the isovector channel of the nuclear interaction [17–21].

Effective mass of nucleon quantifies the momentum dependence of nuclear force in the medium. It can be quoted for infinite nuclear matter at the Fermi surface. It is, however, necessary to realize that the concept of effective mass is different in non-relativistic [22, 23] and relativistic formalism [24]. Nevertheless, it plays some crucial roles to determine various finite nuclear properties *e.g.* isoscalar giant quadrupole resonance (ISGQR) [25], nucleon nucleon scattering in optical potentials [26] or even in realizing various properties of nuclear matter and neutron stars [27, 28]. Recently, a systematic study was performed using RMF models which assessed the impact of relativistic (Dirac) effective mass (M^*) on the properties of neutron star [29]. The isovector splitting of the effective mass, which measures the difference between neutron (M_n^*) and proton (M_p^*) effective mass, can influence greatly as well the physical properties of finite nuclei such as locating the drip-lines [30] or nucleon-nucleus scattering of asymmetric systems [26]. Its impact increases manifold in high density environment which can alter thermal and transport properties of asymmetric matter [31, 32] or neutrino opacities of neutron star matter [33]. To settle its value, even at saturation, remains a persisting challenge both theoretically [34–38] and experimentally [26, 39, 40].

Appearance of isovector splitting of effective mass to the leading order in RMF models occurs through the isovector-scalar δ mesons. It impacts the proton fraction in neutron stars and hence the cooling process of

* virenthakur2154@gmail.com

† raj.phy@gmail.com

‡ sinp.bijay@gmail.com

§ shashi.dhiman@gmail.com

neutron stars after formation [41, 42]. It can also influence the global properties of neutron stars [27, 28, 43–46]. A systematic study of RMF models with added freedom in the isospin channel through δ meson, optimized using well constrained finite nuclear properties and extrapolating at high density to understand the properties of neutron stars and in general dense matter EoS, can enhance our knowledge on the density dependence of the isovector channel of nuclear interaction.

The present study is aimed towards investigating the effects of δ meson on the dense matter EoS within the framework of RMF model. We generate several parameter sets by varying the coupling strength of δ meson to the nucleons such that the low density behaviour of the EOSs remain consistent with the available finite nuclei data and a few empirical properties of infinite nuclear matter evaluated at the saturation density. The properties of neutron stars obtained with these EOSs are then compared to assess the role of δ mesons.

The paper is organized as follows. In section II, the theoretical framework which is used to construct the EoS for neutron stars is discussed. We also discuss the procedure to optimize the coupling constants and the method to perform a covariance analysis in the same section. In section III, we present our results. We summarize and draw our conclusions in section IV.

II. FORMALISM

A. Theoretical model

The Lagrangian density for the RMF model used in the present study based on different non-linear, self and inter-couplings among isoscalar-scalar σ , isoscalar-vector ω_μ , isovector-scalar δ and isovector-vector ρ_μ meson fields and nucleonic Dirac field Ψ [47, 48], is given by

$$\begin{aligned} \mathcal{L} = & \sum_q \bar{\Psi} [i\gamma^\mu \partial_\mu - (M - g_\sigma \sigma - g_\delta \delta \cdot \tau) \\ & - (g_\omega \gamma^\mu \omega_\mu + \frac{1}{2} g_\rho \gamma^\mu \tau \cdot \rho_\mu)] \Psi + \frac{1}{2} (\partial_\mu \sigma \partial^\mu \sigma - m_\sigma^2 \sigma^2) \\ & - \frac{\bar{\kappa}}{3!} g_\sigma^3 \sigma^3 - \frac{\bar{\lambda}}{4!} g_\sigma^4 \sigma^4 - \frac{1}{4} \omega_{\mu\nu} \omega^{\mu\nu} + \frac{1}{2} m_\omega^2 \omega_\mu \omega^\mu \\ & + \frac{1}{4!} \zeta g_\omega^4 (\omega_\mu \omega^\mu)^2 - \frac{1}{4} \rho_{\mu\nu} \rho^{\mu\nu} + \frac{1}{2} m_\rho^2 \rho_\mu \rho^\mu \\ & + \frac{1}{2} (\partial_\mu \delta \partial^\mu \delta - m_\delta^2 \delta^2) + \frac{1}{2} c_1 g_\omega^2 g_\rho^2 \omega_\mu \omega^\mu \rho_\mu \rho^\mu. \end{aligned} \quad (1)$$

The Dirac effective mass for the nucleons (q) appearing in the Lagrangian density above is specified as

$$M_q^* = (M - g_\sigma \sigma - g_\delta \delta \cdot \tau), \quad (2)$$

where, $\tau = 1(-1)$ for $q =$ neutron (proton). Following the Euler-Lagrange formalism one can readily find the expressions for energy density \mathcal{E} and pressure P as a function of density from Eq. (1) [49].

B. Optimization and covariance analysis

In the present study, five new relativistic interactions SRV00, SRV01, SRV02, SRV03, and SRV04 have been generated for the Lagrangian density given by Eq. (1) to investigate the effect of δ meson on the properties of finite nuclei and neutron star matter. Here, SRV00, SRV01, SRV02, SRV03 and SRV04 parametrizations correspond to different value of the coupling of δ -meson to the nucleon i.e. $g_\delta = 0.0, 1.0, 2.0, 3.0$ and 4.0 respectively. As the effect of δ meson is predominantly important at suprasaturation densities, one can *a-priori* anticipate its insignificant impact in finite nuclei, which is primarily sensitive to the EoS at subsaturation densities. This is the reason why we kept fixed the g_δ at aforementioned values optimizing the rest of the parameters in Eq. (1). This is not far from the strategy recently used by Li *et. al.* in Ref. [46]. The parameters of the model are obtained by fitting the experimental data [50] on binding energies (BE) and charge rms radii (r_{ch}) [51] of some spherical nuclei $^{16,24}\text{O}$, $^{40,48}\text{Ca}$, $^{56,78}\text{Ni}$, ^{88}Sr , ^{90}Zr , $^{100,116,132}\text{Sn}$ and ^{208}Pb . For the open shell nuclei, the pairing has been included using BCS formalism with constant pairing gaps [52, 53] that are taken from the nucleon separation energies of neighboring nuclei [50]. Neutron and proton pairing gaps are evaluated by using fourth order finite difference mass formula (five point difference) [54]. The neutron and proton pairing gaps (Δ_n, Δ_p) in MeV for the open shell nuclei are $^{88}\text{Sr}(0.0, 1.284)$, $^{90}\text{Zr}(0.0, 1.239)$ and $^{116}\text{Sn}(1.189, 0.0)$. The neutron pairing gap for ^{24}O practically vanishes since the first unoccupied orbit $1d_{3/2}$ is almost 4.5 MeV above the completely filled $2s_{1/2}$ orbit [55, 56]. The pairing correlation energies for a fix gap Δ is calculated by using the pairing window of $2\hbar\omega$, where $\hbar\omega = 45A^{-1/3} - 25A^{-2/3}$ MeV [48]. We also incorporated the recently measured neutron skin thickness of ^{208}Pb using the parity violating electron scattering experiment [15] in our fit data.

The optimization of the parameters (\mathbf{p}) appearing in the Lagrangian (Eq. 1) is done by using the simulated annealing method (SAM) [57–59] by following χ^2 minimization procedure which is given as,

$$\chi^2(\mathbf{p}) = \frac{1}{N_d - N_p} \sum_{i=1}^{N_d} \left(\frac{M_i^{exp} - M_i^{th}}{\sigma_i} \right)^2, \quad (3)$$

where N_d is the number of experimental data points and N_p is the number of fitted parameters. The σ_i denotes adopted errors [60, 61] and M_i^{exp} and M_i^{th} are the experimental and the corresponding theoretical values, respectively, for a given observable. The minimum value of χ_0^2 corresponds to the optimal values \mathbf{p}_0 of the parameters.

Once the optimized parameter set is obtained, the correlation coefficient between two quantities Y and Z, can be calculated by covariance analysis [60–64] as

$$r_{YZ} = \frac{\overline{\Delta Y \Delta Z}}{\sqrt{\overline{\Delta Y^2} \overline{\Delta Z^2}}}, \quad (4)$$

TABLE I. SRV parameter sets for the Lagrangian of RMF model as given in Eq.(1). The parameter $\bar{\kappa}$ is in fm^{-1} . The values of meson masses m_σ , m_ω , m_ρ and m_δ are in MeV. The nucleonic mass (M) and meson masses (m_ω , m_ρ and m_δ) are taken as 939, 782.5, 762.468 and 980 MeV, respectively. The values of $\bar{\kappa}$, $\bar{\lambda}$, and c_1 are multiplied by 10^2 .

Parameters	SRV00	SRV01	SRV02	SRV03	SRV04
g_σ	10.3109±0.1109	10.3442±0.0978	10.3344±0.1135	10.3723±0.0999	10.3735±0.1294
g_ω	13.1772±0.1621	13.2508±0.1379	13.2137±0.1414	13.3113±0.1269	13.2984±0.1815
g_ρ	10.8834±1.1730	11.2832±1.0110	11.5834±0.9676	12.4834±1.1274	13.1833±0.8043
$\bar{\kappa}$	1.8509±0.0500	1.8624±0.0700	1.8780±0.0200	1.8242±0.0500	1.8490±0.0800
$\bar{\lambda}$	-0.05151±0.0700	-0.05803±0.0600	-0.06060±0.0600	-0.04934±0.0800	-0.05621±0.0800
ζ	0.02116±0.0017	0.02050±0.0013	0.02017±0.0011	0.02177±0.0012	0.02089±0.0027
c_1	4.60038±2.3600	4.49219±1.9200	4.20853±1.5600	3.66169±1.4900	3.01068±0.8800
m_σ	501.9596±0.9230	501.0200±1.0071	501.6638 ±1.3141	500.7480±1.2629	501.0215±1.3663

where covariance between Y and Z is expressed as

$$\overline{\Delta Y \Delta Z} = \sum_{\alpha\beta} \left(\frac{\partial Y}{\partial p_\alpha} \right)_{\mathbf{p}_0} C_{\alpha\beta}^{-1} \left(\frac{\partial Z}{\partial p_\beta} \right)_{\mathbf{p}_0}. \quad (5)$$

Here, $C_{\alpha\beta}^{-1}$ is an element of inverted curvature matrix given by

$$C_{\alpha\beta} = \frac{1}{2} \left(\frac{\partial^2 \chi^2(\mathbf{p})}{\partial p_\alpha \partial p_\beta} \right)_{\mathbf{p}_0}. \quad (6)$$

The standard deviation, $\overline{\Delta Y^2}$, in Y can be computed using Eq. (5) by substituting Z = Y.

III. RESULTS AND DISCUSSION

We have obtained five different parameter sets corresponding to different values of g_δ by calibrating the remaining parameters to a suitable set of on finite nuclei as described earlier. All parametrizations obtained in the present work give equally good fit to the properties of finite nuclei which were used for the optimization procedure. In Table I we display optimum values of the model parameters for all the five SRV parameter sets along with the uncertainties on them computed using Eq. (5). It can be seen that the parameter g_ρ increases with the increase in value of g_δ . A larger value of g_ρ is required in the presence of the δ -field to fit the properties of finite nuclei. As the contribution of the δ -field is attractive, increased binding due to the δ -field has to be compensated by the higher value of the repulsion by the ρ -field. The parameter g_ρ has its lowest value for SRV00 parametrization ($g_\delta=0$). For any finite value of δ -coupling ($g_\delta > 0$) i.e. for SRV01, SRV02, SRV03 and SRV04 parametrizations, the strength of ρ -coupling (g_ρ) increases gradually. The cross-coupling between the ω_μ and ρ_μ fields quantified by the term c_1 decreases slightly from 4.6003 to 3.0107 as the value of coupling constant g_δ increases from 0.0 to 4.0 corresponding to different SRV parametrizations.

In Table II, different observables fitted in the present work, their experimental values [50, 51], adopted errors σ on them [65] along with the calculated values for different

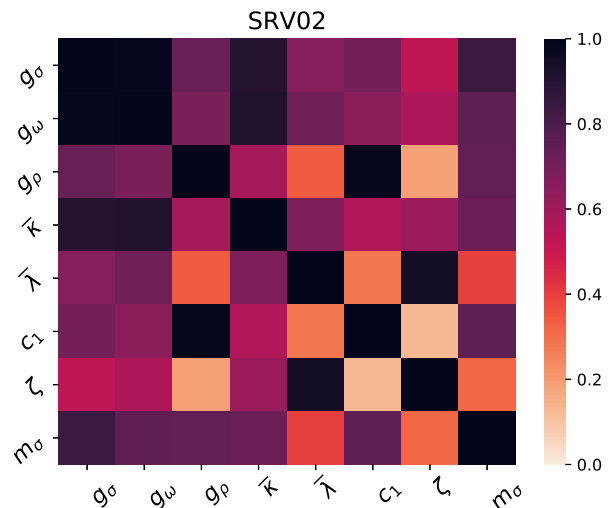


FIG. 1. (Color online) Correlation coefficients (absolute values) among the model parameters for SRV02 parametrization for the Lagrangian given by Eq. (1).

SRV parametrizations are displayed. The estimated uncertainties are also listed for the fitted observables. The fitted values of finite nuclei properties are quite close to their experimental counterparts. The root mean square (rms) errors on the BE are found to be in the range 1.50–1.86 MeV, and the ones for r_{ch} are found to be 0.02 fm for the different parameterizations. It is quite interesting to observe that even though g_δ influences the coupling g_ρ , the isovector sensitive observable Δr_{np} varies only slightly ~ 0.01 fm across the different SRV models obtained in the present work. This observation is quite similar to the one obtained by Li *et. al.* [46].

In Table III, we present the results for the properties of Symmetric Nuclear Matter (SNM) such as binding energy per nucleon (E/A), incompressibility (K), the ratio of effective mass to the mass of nucleon (M^*/M) along with symmetry energy coefficient (J), and its slope (L), all are evaluated at the saturation density (ρ_0). We also quote the theoretically calculated error on them. The results are presented for all five SRV parametrizations.

TABLE II. The values of binding energy (BE) and charge radii (r_{ch}) of fitted nuclei along with theoretical errors obtained for different SRV parametrizations. The corresponding experimental values [50, 51] are also listed. The value of neutron skin thickness (Δr_{np}) for ^{208}Pb is given along with the experimental data [15]. The adopted errors on the observables (σ) used for optimisation of parameters are also displayed. The value of BE are given in units of MeV and r_{ch} and Δr_{np} are in fm.

Nucleus	Observables	Exp.	σ	SRV00	SRV01	SRV02	SRV03	SRV04
^{16}O	BE	127.62	4.0	128.67 \pm 0.52	128.83 \pm 0.50	128.94 \pm 0.55	128.90 \pm 0.51	128.94 \pm 0.61
	r_{ch}	2.699	0.04	2.709 \pm 0.008	2.712 \pm 0.023	2.711 \pm 0.031	2.710 \pm 0.013	2.710 \pm 0.023
^{24}O	BE	168.96	1.0	169.95 \pm 0.96	169.38 \pm 0.90	169.64 \pm 0.89	168.90 \pm 1.01	169.00 \pm 0.93
^{40}Ca	BE	342.04	3.0	343.40 \pm 0.69	343.14 \pm 0.65	343.18 \pm 0.53	344.41 \pm 0.63	344.39 \pm 0.91
	r_{ch}	3.478	0.02	3.454 \pm 0.014	3.457 \pm 0.007	3.455 \pm 0.016	3.455 \pm 0.014	3.455 \pm 0.017
^{48}Ca	BE	415.97	1.0	415.59 \pm 0.54	415.15 \pm 0.52	415.37 \pm 0.45	415.37 \pm 0.63	415.48 \pm 0.52
	r_{ch}	3.477	0.02	3.468 \pm 0.016	3.469 \pm 0.014	3.468 \pm 0.014	3.467 \pm 0.014	3.467 \pm 0.022
^{56}Ni	BE	484.01	5.0	482.05 \pm 1.28	482.39 \pm 1.21	482.28 \pm 1.31	483.12 \pm 1.48	483.22 \pm 1.56
	r_{ch}	3.750	0.02	3.712 \pm 0.022	3.709 \pm 0.017	3.708 \pm 0.14	3.707 \pm 0.017	3.705 \pm 0.013
^{78}Ni	BE	642.56	2.0	641.39 \pm 1.03	640.01 \pm 0.97	641.05 \pm 1.01	640.21 \pm 1.08	640.18 \pm 1.07
^{88}Sr	BE	768.42	1.0	768.24 \pm 0.60	767.72 \pm 0.57	767.84 \pm 0.58	768.39 \pm 0.60	768.40 \pm 0.62
	r_{ch}	4.219	0.02	4.226 \pm 0.016	4.227 \pm 0.014	4.227 \pm 0.013	4.225 \pm 0.021	4.225 \pm 0.0146
^{90}Zr	BE	783.81	1.0	783.92 \pm 0.69	783.58 \pm 0.64	783.59 \pm 0.68	784.37 \pm 0.69	784.36 \pm 0.68
	r_{ch}	4.269	0.02	4.280 \pm 0.019	4.280 \pm 0.019	4.280 \pm 0.013	4.278 \pm 0.029	4.278 \pm 0.015
^{100}Sn	BE	825.10	2.0	826.60 \pm 1.28	826.95 \pm 1.24	827.56 \pm 1.14	827.09 \pm 1.23	827.01 \pm 1.66
^{116}Sn	BE	988.67	2.0	988.34 \pm 0.83	987.74 \pm 0.73	987.72 \pm 2.18	988.49 \pm 0.82	988.25 \pm 0.88
	r_{ch}	4.627	0.02	4.617 \pm 0.016	4.618 \pm 0.014	4.617 \pm 0.009	4.615 \pm 0.012	4.615 \pm 0.020
^{132}Sn	BE	1100.22	1.0	1101.38 \pm 0.84	1100.58 \pm 0.80	1101.48 \pm 0.77	1100.59 \pm 0.86	1100.70 \pm 0.82
	r_{ch}	4.709	0.02	4.721 \pm 0.019	4.721 \pm 0.019	4.720 \pm 0.010	4.719 \pm 0.012	4.717 \pm 0.011
^{208}Pb	BE	1636.34	1.0	1636.58 \pm 1.03	1635.98 \pm 0.98	1636.32 \pm 0.96	1636.27 \pm 1.05	1636.10 \pm 1.02
	r_{ch}	5.501	0.02	5.530 \pm 0.015	5.531 \pm 0.014	5.529 \pm 0.014	5.527 \pm 0.021	5.526 \pm 0.011
	Δr_{np}	0.283 \pm 0.071	0.071	0.222 \pm 0.032	0.223 \pm 0.028	0.217 \pm 0.026	0.215 \pm 0.035	0.214 \pm 0.029

TABLE III. The bulk nuclear matter properties at saturation density for SRV parametrizations are listed: ρ_0 , E/A, K, J, L and M^*/M denotes the saturation density, binding energy per nucleon, incompressibility coefficient, symmetry energy, the slope of symmetry energy, and the ratio of effective nucleon mass to the nucleon mass, respectively.

Parameters	SRV00	SRV01	SRV02	SRV03	SRV04
ρ_0 (fm^{-3})	0.149 \pm 0.003	0.149 \pm 0.002	0.149 \pm 0.002	0.149 \pm 0.003	0.149 \pm 0.008
E/A (MeV)	-16.11 \pm 0.06	-16.11 \pm 0.05	-16.09 \pm 0.05	-16.12 \pm 0.06	-16.11 \pm 0.04
K (MeV)	223.94 \pm 8.57	221.78 \pm 9.95	222.05 \pm 5.47	221.72 \pm 10.62	221.11 \pm 23.20
J (MeV)	33.49 \pm 1.82	33.75 \pm 1.77	33.31 \pm 1.78	33.54 \pm 2.13	33.34 \pm 2.08
L (MeV)	65.23 \pm 15.37	63.82 \pm 13.50	61.49 \pm 13.22	58.06 \pm 15.93	55.31 \pm 13.76
M^*/M	0.606 \pm 0.013	0.602 \pm 0.010	0.603 \pm 0.005	0.601 \pm 0.009	0.600 \pm 0.009

The value of E/A lies in the range -16.09 to -16.12 for the five parametrizations. The value of J and L obtained by our parametrizations are consistent with the constraints from observational analysis $J = 31.6 \pm 2.66$ MeV and $L = 58.9 \pm 16$ MeV [66, 67]. The value of K is also in agreement with the value 240 ± 20 MeV determined from isoscalar giant monopole resonance (IS-GMR) for ^{90}Zr and ^{208}Pb nuclei [68, 69]. It can also be seen from Table III that the mean values of the slope of symmetry energy (L) for SRV parametrizations decrease with the increase in the value of g_δ . The average value of L decreases from 65.23 MeV in SRV00 to 55.31 MeV for SRV04. It can be noted that the isoscalar properties (E/A, K, ρ_0 and M^*/M) are well constrained for all SRV parametrizations. The only exception is the error on K in case of SRV04, where the error is almost 10% of its central value. But in the isovector sector, the percentage error on the slope of symmetry energy (L) are consis-

tently on the larger side for all SRV parametrizations.

A great deal of importance to perform covariance analysis in theoretical studies has been pointed out recently [60, 63]. It not only enables one to quote statistical uncertainties on model parameters or any calculated observables, but also provides complementary information about the sensitivity of the parameters to physical observables, redundancies among fitted observables or interdependences among model parameters. As our primary objective is not to establish an ultimate model, for demonstrative purpose, we will discuss the results of covariance analysis as outlined in Section IIB, only for the model SRV02. The results for other parameter sets are quite similar (not shown here). In Fig. 1, the correlation coefficients between different model parameters appearing in Eq. (1) are outlined for SRV02 parametrization. A strong correlation is found between the several pairs of model parameters, like, g_σ and g_ω , g_ρ and c_1 and $\bar{\lambda}$

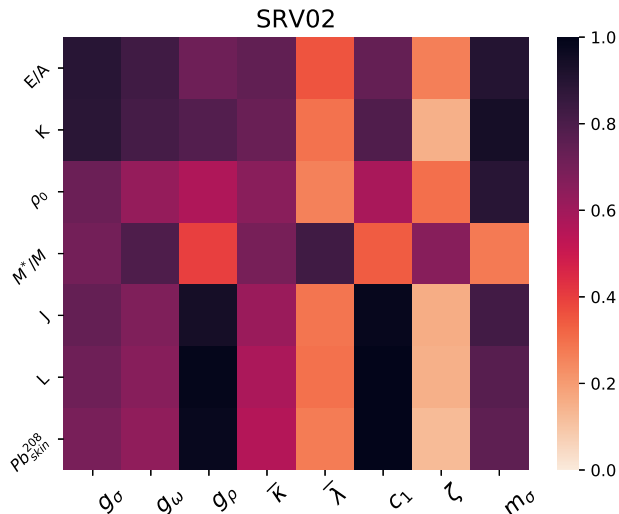


FIG. 2. (Color online) Correlation coefficients (absolute values) between the model parameters and a set of physical observables for SRV02 parametrization (see text for details).

and ζ with correlation coefficients 0.99, 0.98 and 0.95, respectively. These interdependences mean that if one of these pairs are fixed at a particular value, the other must attain the precise value as suggested by their correlation to satisfactorily obtain the fit data. The results obtained for the correlations among model parameters presented in Fig. 1 are quite similar to the obtained in Refs. [19, 70]. Anticipating the strong correlation between L and Δr_{np} which is shown later (see Fig. 3), this may be attributed to the large experimental error on the Δr_{np} for ^{208}Pb , which also led us choosing a rather large adopted error during optimization. The theoretical errors on the Δr_{np} of ^{208}Pb nucleus are found to be 0.032, 0.028, 0.026, 0.0353 and 0.029 fm for SRV00, SRV01, SRV02, SRV03, and SRV04 parametrizations, respectively. These are much smaller compared to the adopted error (0.071 fm, which is also the experimental error obtained in Ref. [15]).

We now display in Fig. 2, the correlation coefficients between the model parameters appearing in Lagrangian (Eq. 1) and the different properties of interest corresponding to the SNM and the density dependent symmetry energy as displayed in Table III and the Δr_{np} of ^{208}Pb for SRV02. A strong correlation is observed between the isovector parameter g_ρ with the symmetry energy coefficient (J), its slope (L) and Δr_{np} of ^{208}Pb . The vector mixing parameter c_1 is also found to have a strong correlation with the J and L. This strong correlation is anticipated, as c_1 and g_ρ are strongly correlated to each other, which was observed in Fig. 1. It is also realized from Fig. 2 that bulk properties of SNM like E/A, K, ρ_0 and M^*/M have strong correlations with isoscalar coupling parameters g_σ , g_ω and $\bar{\kappa}$. This study is quite consistent with previous calculations in the literature [20, 56, 70].

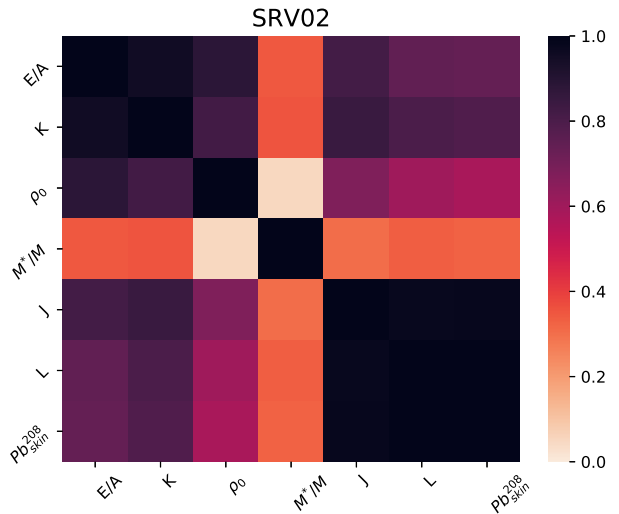


FIG. 3. (Color online) Correlation coefficients (absolute values) for few bulk nuclear matter properties and neutron skin of ^{208}Pb for SRV02 parametrization.

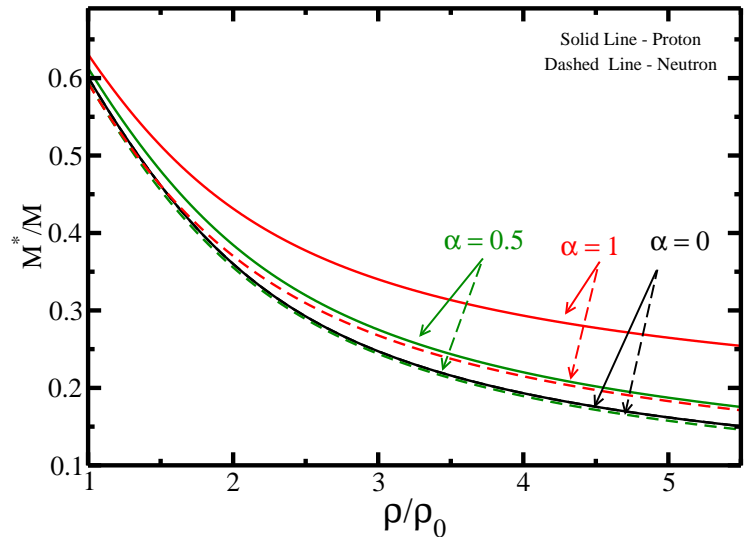


FIG. 4. (Color online) Effective masses of proton and neutron for a few values of asymmetry parameter α for SRV04 parametrization.

In Fig. 3, we display the correlation coefficients among the different observables in graphical form, particularly which were also studied in Fig. 2. In the isoscalar sector the only strong correlation observed is between binding energy per nucleon (E/A) and incompressibility coefficient (K). The K also shows some mild correlations with all other observables displayed in the figure. The symmetry energy J and its slope parameter L are found to be strongly correlated. As mentioned earlier in the discussion of Table III, we observe a strong correlation of the neutron skin thickness of ^{208}Pb with J and L. These results are also in line with the earlier ones [70].

It is quite important to emphasize that we kept fixed the strength of the coupling of δ meson to different values and optimized the rest. This might be partially responsible to impart a strong correlation among the isovector sensitive parameters g_ρ, c_1 to J, L or Δr_{np} of ^{208}Pb (see Fig. 2) to reproduce the fitted data within bounds. It further gets clarified in the strong correlations among Δr_{np} (^{208}Pb), J and L in Fig. 3. Anticipating the results obtained for neutron stars which are discussed later, this strong correlation somewhat restricts the behavior of the matter at high densities in the isovector channel, resulting in a monotonic increasing in the radius and tidal deformability of $1.4 M_\odot$ (see Table IV) with the increase of the δ meson coupling g_δ . A full optimization is thus needed with suitable data in the future including g_δ , to understand this behavior further. In the present work we have included the simplest form of δ -meson coupling (g_δ) to the nucleons. Furthermore, a higher order mixed scalar interactions of δ meson has a large influence on the symmetry energy and its density dependence. This enables one to have flexibility to vary the behaviour of EoS at high density and gives a large influence on the properties of neutron stars [71–73]. To study the effects of δ -meson on nucleon mass, in Fig. 4, the effective mass of proton and neutron are plotted as a function of baryon density for three values of asymmetry parameter $\alpha = 0, 0.5, 1$ ($\alpha = \frac{\rho_n - \rho_p}{\rho_n + \rho_p}$) for SRV04 parametrization, which has the largest value of g_δ amongst all SRV variants obtained in the present work. The asymmetry parameter $\alpha = 0.0$ represents the SNM and $\alpha = 1$ corresponds to the pure neutron matter (PNM). It is clear from the Eq. (2) that the presence of δ -meson leads to splitting of nucleon mass. For SNM, there is no splitting of the nucleon mass. In Fig. 4, the solid (dashed) lines depict the effective mass of proton (neutron) for $\alpha = 0, 0.5$ and 1.0 . One can observe from the figure that the effective proton mass is larger than the neutron effective mass. The splitting of the proton and neutron effective masses due to the δ -meson can be important in the highly asymmetric system like a neutron star or supernova environment. At the center of a neutron star the density can reach $\sim 5\text{--}6 \rho_0$ and $\alpha \sim 0.7\text{--}0.8$. One can readily estimate the amount of splitting in the effective mass in this situation looking at Fig. 4. It can also affect the transport properties of neutron star matter [74].

To assess the impact of δ -meson on the global properties of neutron star, we plot the gravitational mass (M_G) of non-rotating neutron star as a function of radius for all SRV parametrizations in Fig. 5. The maximum mass (M_{max}) and the corresponding radius (R_{max}) of neutron star for all the models obtained here lie in the range $2.04\text{--}2.13 M_\odot$ and $11.48\text{--}12.11$ km, respectively. This satisfies the recently measured radius of PSRJ0740+6620 with $12.45^{+0.65}_{-0.65}$ km by NICER collaboration [12, 13]. The radius of neutron star of $2M_\odot$ is also in accordance with the observational data of PSRJ0740+6620 by NICER [12, 13]. The maximum mass of the neutron star attained by various SRV parametrizations supports the constraint

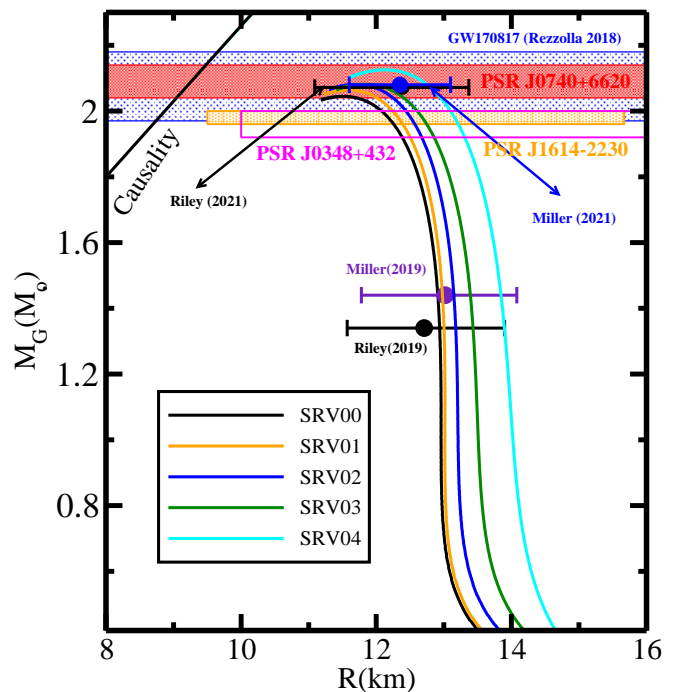


FIG. 5. (Color online) Mass-Radius relation of neutron star for SRV parametrizations.

from PSRJ0740+6620 with the mass of $2.08 \pm 0.07 M_\odot$ [75, 76]. It is observed that the radius ($R_{1.4}$) of neutron star with mass $1.4M_\odot$, can be significantly affected by the presence of δ -meson as we move from parametrization set SRV00 to SRV04. The value of $R_{1.4}$ with the inclusion of TM1 crust EoS [77] lies in the range $12.92\text{--}13.86$ km, which is also in line with the range proposed in Ref. [12, 78]. It is observed that the radius $R_{1.4}$ increases by 7.27% and the maximum mass of neutron star changes by 4.4% from SRV00 to SRV04 parametrizations with the variation of coupling $g_\delta = 0.0$ to 4.0 . This change in the neutron star properties may be attributed to the impact of δ -meson, which affects high-density behavior of asymmetric nuclear matter.

Tidal deformability imparted by the companion stars on one another in a binary system can yield remarkable information on the EoS for neutron star [79, 80]. In Fig. 6, we show the results of dimensionless tidal deformability Λ , defined as $\Lambda = (2/3)k_2(R/M_G)^5$, where k_2 is the love number, as a function of the neutron star mass M_G for different SRV models. The recent constraints on the tidal deformability $\Lambda_{1.4}$ of $1.4M_\odot$ neutron star including GW170817 [8, 81] is also given in the figure. The value of $\Lambda_{1.4}$ lies in the range $484\text{--}783$ for different SRV parametrizations, which satisfies the proposed limit are listed in Refs. [8, 78, 82, 83]. The value of $\Lambda_{1.4}$ increases with the increase in the value of the coupling g_δ corresponding to the SRV parametrizations as can be seen from Fig. 6. All these results are summarized in Table IV. The theoretical errors/uncertainties in neutron star properties for SRV parametrizations are also mentioned

TABLE IV. The properties of nonrotating neutron star for the various EOSs computed with SRV parameter sets are presented along with the theoretical errors on them. M_G and R_{max} denote the Maximum Gravitational mass and corresponding radius. The values for $R_{1.4}$ and $\Lambda_{1.4}$ denote radius and dimensionless tidal deformability at $1.4M_\odot$.

No.	EOS	M_G (M_\odot)	R_{max} (km)	$R_{1.4}$ (km)	$R_{2.0}$ (km)	$\Lambda_{1.4}$
1.	SRV00	2.04 ± 0.03	11.48 ± 0.08	12.92 ± 0.22	12.07 ± 0.31	484.16 ± 62.10
2.	SRV01	2.06 ± 0.02	11.55 ± 0.13	12.99 ± 0.20	12.24 ± 0.21	504.95 ± 58.02
3.	SRV02	2.07 ± 0.02	11.67 ± 0.07	13.16 ± 0.13	12.43 ± 0.14	565.52 ± 60.33
4.	SRV03	2.08 ± 0.02	11.81 ± 0.11	13.41 ± 0.21	12.60 ± 0.16	652.60 ± 52.01
5.	SRV04	2.13 ± 0.06	12.11 ± 0.23	13.86 ± 0.21	13.09 ± 0.33	783.96 ± 70.03

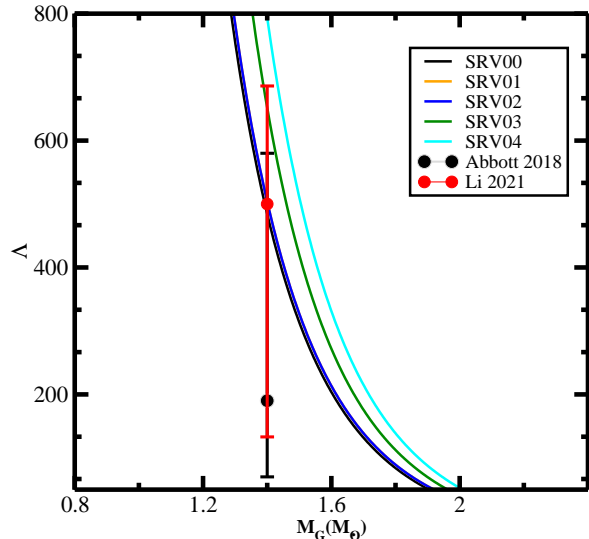


FIG. 6. (Color online) Variation of dimensionless tidal deformability (Λ) with respect to gravitational mass for SRV parametrizations.

in the table. The neutron star properties such as M_{max} , R_{max} , $R_{1.4}$, $R_{2.0}$ are relatively well constrained for all SRV parametrizations (at $\leq 3\%$) whereas for $\Lambda_{1.4}$, the theoretical uncertainties are found to be $\leq 10\%$.

To this end, we may mention that the contribution of δ meson is considered only through its linear interaction with nucleons. However, inclusion of the self interaction of δ mesons and the mixed interactions with other mesons may alter the symmetry energy at suprasaturation densities. This would further enhance the flexibility of EOS of dense matter and accordingly the properties of neutron stars [71–73]. Inclusion of the higher order contributions of δ meson thus enable one to model the properties of neutron stars in somewhat independent of the properties of finite nuclei. The optimization of effective Lagrangian that includes different terms involving δ meson field requires accurate knowledge of neutron star properties over a wide range of mass.

IV. SUMMARY AND CONCLUSIONS

The effect of the isovector-scalar field corresponding to δ -meson in relativistic mean field theory is investigated. We have generated five sets of SRV parametrizations SRV00, SRV01, SRV02, SRV03 and SRV04 to explore the effects of δ -meson on the properties of finite nuclei, infinite nuclear matter, and neutron stars. A covariance analysis to measure the accuracy of model predictions is also performed. This also enabled us to carry out a systematic study of correlations among model parameters and various finite nuclei and infinite nuclear matter properties of interest. The SRV parametrizations have been obtained in such a way that they reproduce the ground state properties of the finite nuclei and infinite nuclear matter properties quite convincingly. In turn, they satisfy the constraints on mass and radius of the neutron star and its dimensionless tidal deformability, Λ , from recent astrophysical observations [8, 66, 67, 78, 81]. It is observed that to fit the properties of finite nuclei and infinite nuclear matter, a stronger coupling between the ρ -meson and nucleons (g_ρ) is required in the presence δ -meson field. Furthermore, the δ -meson significantly affects the radius of canonical neutron star. It is found that the contributions from δ -meson is important and has some significant effects on the dense matter EoS. The value of $\Lambda_{1.4}$ for different SRV parametrization is also in line with the constraint obtained from GW170817 event. It is clear that the isovector splitting of effective mass of nucleon in the presence of δ in dense asymmetric matter, like the scenario present in the core of a neutron star, can be significant. It remains, however, an open question how to identify in future the signatures of isovector effective mass splitting from astrophysical observations.

ACKNOWLEDGMENTS

Virender Thakur is highly thankful to Himachal Pradesh University and DST-INSPIRE (Govt. of India) for providing computational facility and financial assistance (Junior/Senior Research Fellowship under grant number “DST/INSPIRE Fellowship/2017/IF170302”). C.M. acknowledges partial support from the IN2P3 Master Project “NewMAC”.

-
- [1] JD Walecka. A theory of highly condensed matter. *Annals of Physics*, 83(2):491–529, 1974.
- [2] NK Glendenning and SA Moszkowski. Reconciliation of neutron-star masses and binding of the λ in hypernuclei. *Physical review letters*, 67(18):2414, 1991.
- [3] M. Dutra, O. Lourenço, S. S. Avancini, B. V. Carlson, A. Delfino, D. P. Menezes, C. Providência, S. Typel, and J. R. Stone. Relativistic mean-field hadronic models under nuclear matter constraints. *Phys. Rev. C*, 90:055203, 2014.
- [4] M. Oertel, M. Hempel, T. Klähn, and S. Typel. Equations of state for supernovae and compact stars. *Rev. Mod. Phys.*, 89:015007, Mar 2017.
- [5] X. Roca-Maza and N. Paar. Nuclear equation of state from ground and collective excited state properties of nuclei. *Prog. Part. Nucl. Phys.*, 101:96–176, 2018.
- [6] P. B. Demorest, Tim Pennucci, S. M. Ransom, M. S. E. Roberts, and J. W. T. Hessels. A two-solar-mass neutron star measured using Shapiro delay. *nature*, 467(7319):1081, 2010.
- [7] John Antoniadis, Paulo C. C. Freire, Norbert Wex, Thomas M Tauris, Ryan S Lynch, Marten H van Kerkwijk, Michael Kramer, Cees Bassa, Vik S Dhillon, Thomas Driebe, et al. A massive pulsar in a compact relativistic binary. *Science*, 340(6131):1233232, 2013.
- [8] B. P. Abbott, R. Abbott, T. D. Abbott, F. Acernese, K. Ackley, C. Adams, T. Adams, P. Addesso, R. X. Adhikari, V. B. Adya, et al. Gw170817: Measurements of neutron star radii and equation of state. *Phys. Rev. Lett.*, 121(16):161101, 2018.
- [9] B. P. Abbott, R. Abbott, T. D. Abbott, F. Acernese, K. Ackley, C. Adams, T. Adams, P. Addesso, R. X. Adhikari, V. B. Adya, et al. Properties of the binary neutron star merger gw170817. *Phys. Rev. X*, 9(1):011001, 2019.
- [10] M. C. Miller, F. K. Lamb, A. J. Dittmann, S. Bogdanov, Z. Arzoumanian, K. C. Gendreau, S. Guillot, A. K. Harding, W. C. G. Ho, J. M. Lattimer, R. M. Ludlam, S. Mahmoodifar, S. M. Morsink, P. S. Ray, T. E. Strohmayer, K. S. Wood, T. Enoto, R. Foster, T. Oka-jima, G. Prigozhin, and Y. Soong. PSR j0030+0451 mass and radius from NICER data and implications for the properties of neutron star matter. *The Astrophysical Journal*, 887(1):L24, dec 2019.
- [11] T. E. Riley, A. L. Watts, S. Bogdanov, P. S. Ray, R. M. Ludlam, S. Guillot, Z. Arzoumanian, C. L. Baker, A. V. Bilous, D. Chakrabarty, K. C. Gendreau, A. K. Harding, W. C. G. Ho, J. M. Lattimer, S. M. Morsink, and T. E. Strohmayer. A NICER view of PSR j0030+0451: Millisecond pulsar parameter estimation. 887:L21, 2019.
- [12] MC Miller, FK Lamb, AJ Dittmann, S Bogdanov, Z Arzoumanian, KC Gendreau, S Guillot, WCG Ho, JM Lattimer, M Loewenstein, et al. The radius of psr j0740+6620 from nicer and xmm-newton data. *arXiv preprint arXiv:2105.06979*, 2021.
- [13] Thomas E Riley, Anna L Watts, Paul S Ray, Slavko Bogdanov, Sebastien Guillot, Sharon M Morsink, Anna V Bilous, Zaven Arzoumanian, Devarshi Choudhury, Julia S Deneva, et al. A nicer view of the massive pulsar psr j0740+6620 informed by radio timing and xmm-newton spectroscopy. *The Astrophysical Journal Letters*, 918(2):L27, 2021.
- [14] J.M. Lattimer. Neutron stars and the nuclear matter equation of state. *Annual Review of Nuclear and Particle Science*, 71(1):433–464, 2021.
- [15] D Adhikari, H Albataineh, D Androic, K Aniol, DS Armstrong, T Averett, C Ayerbe Gayoso, S Barcus, V Bellini, RS Beminiwattha, et al. Accurate determination of the neutron skin thickness of pb 208 through parity-violation in electron scattering. *Physical review letters*, 126(17):172502, 2021.
- [16] D. Adhikari and et al. *arXiv:2205.11593*, 2022.
- [17] Reed Essick, Ingo Tews, Philippe Landry, and Achim Schwenk. Astrophysical Constraints on the Symmetry Energy and the Neutron Skin of Pb208 with Minimal Modeling Assumptions. *Phys. Rev. Lett.*, 127(19):192701, 2021.
- [18] Paul-Gerhard Reinhard, Xavier Roca-Maza, and Witold Nazarewicz. Information content of the parity-violating asymmetry in ^{208}Pb . *Phys. Rev. Lett.*, 127:232501, Nov 2021.
- [19] C. Mondal. Density dependence of symmetry energy and neutron skin thickness revisited using relativistic mean field models with nonlinear couplings. *Phys. Rev. C*, 105:034305, Mar 2022.
- [20] Paul-Gerhard Reinhard, Xavier Roca-Maza, and Witold Nazarewicz. Combined theoretical analysis of the parity-violating asymmetry for ^{48}Ca and ^{208}Pb . *arXiv:2206.03134v1*, 2022.
- [21] Esra Yüksel and Nils Paar. Implications of parity-violating electron scattering experiments on ^{48}Ca (crex) and ^{208}Pb (prex-ii) for nuclear energy density functionals. *arXiv:2206.06527v1*, 2022.
- [22] Brian D. Serot and John Dirk Walecka. The relativistic nuclear many body problem. *Adv. Nucl. Phys.*, 16:1–327, 1986.
- [23] Lie-Wen Chen, Che Ming Ko, and Bao-An Li. Isospin-dependent properties of asymmetric nuclear matter in relativistic mean field models. *Phys. Rev. C*, 76:054316, 2007.
- [24] M. Jaminon and C. Mahaux. Effective masses in relativistic approaches to the nucleon-nucleus mean field. *Phys. Rev. C*, 40:354–367, Jul 1989.
- [25] X. Roca-Maza, M. Brenna, B. K. Agrawal, P. F. Bortignon, G. Colò, Li-Gang Cao, N. Paar, and D. Vretenar. Giant quadrupole resonances in 208pb, the nuclear symmetry energy, and the neutron skin thickness. *Phys. Rev. C*, 87:034301, 2013.
- [26] Xiao-Hua Li, Wen-Jun Guo, Bao-An Li, Lie-Wen Chen, Farrukh J. Fattoyev, and William G. Newton. Neutron-proton effective mass splitting in neutron-rich matter at normal density from analyzing nucleon-nucleus scattering data within an isospin dependent optical model. *Phys. Lett. B*, 743:408 – 414, 2015.
- [27] Tuhin Malik, C. Mondal, B. K. Agrawal, J. N. De, and S. K. Samaddar. Nucleon effective mass and its isovector splitting. *Phys. Rev. C*, 98(6):064316, 2018.
- [28] Tuhin Malik, B. K. Agrawal, J. N. De, S. K. Samaddar, C. Providência, C. Mondal, and T. K. Jha. Tides in merging neutron stars: Consistency of the gw170817 event with experimental data on finite nuclei. *Phys. Rev. C*, 99:052801, May 2019.

- [29] Suprovo Ghosh, Debarati Chatterjee, and Jürgen Schaffner-Bielich. Imposing multi-physics constraints at different densities on the neutron Star Equation of State. *Eur. Phys. J. A*, 58(3):37, 2022.
- [30] P. J. Woods and C. N. Davids. Nuclei beyond the proton drip-line. *Annual Review of Nuclear and Particle Science*, 47(1):541–590, 1997.
- [31] Bao-An Li, Champak B. Das, Subal Das Gupta, and Charles Gale. Momentum dependence of the symmetry potential and nuclear reactions induced by neutron-rich nuclei at ria. *Phys. Rev. C*, 69:011603, Jan 2004.
- [32] Jun Xu, Lie-Wen Chen, and Bao-An Li. Thermal properties of asymmetric nuclear matter with an improved isospin- and momentum-dependent interaction. *Phys. Rev. C*, 91:014611, Jan 2015.
- [33] M. Baldo, G. F. Burgio, H.-J. Schulze, and G. Taranto. Nucleon effective masses within the brueckner-hartree-fock theory: Impact on stellar neutrino emission. *Phys. Rev. C*, 89:048801, Apr 2014.
- [34] W. Zuo, L. G. Cao, B. A. Li, U. Lombardo, and C. W. Shen. Isospin splitting of the nucleon mean field. *Phys. Rev. C*, 72:014005, Jul 2005.
- [35] E. N. E. van Dalen, C. Fuchs, and Amand Faessler. Effective nucleon masses in symmetric and asymmetric nuclear matter. *Phys. Rev. Lett.*, 95:022302, Jul 2005.
- [36] D. Bandyopadhyay, C. Samanta, S.K. Samaddar, and J.N. De. Thermostatic properties of finite and infinite nuclear systems. *Nuclear Physics A*, 511(1):1–28, 1990.
- [37] C. Mondal, B. K. Agrawal, J. N. De, S. K. Samaddar, M. Centelles, and X. Viñas. Interdependence of different symmetry energy elements. *Phys. Rev. C*, 96:021302, Aug 2017.
- [38] C. Mondal, B. K. Agrawal, J. N. De, and S. K. Samaddar. Correlations among symmetry energy elements in Skyrme models. *Int. J. Mod. Phys. E*, 27(09):1850078, 2018.
- [39] Zhen Zhang and Lie-Wen Chen. Isospin splitting of the nucleon effective mass from giant resonances in ^{208}Pb . *Phys. Rev. C*, 93:034335, Mar 2016.
- [40] Hai-Yun Kong, Jun Xu, Lie-Wen Chen, Bao-An Li, and Yu-Gang Ma. Constraining simultaneously nuclear symmetry energy and neutron-proton effective mass splitting with nucleus giant resonances using a dynamical approach. *Phys. Rev. C*, 95:034324, Mar 2017.
- [41] X Roca-Maza, X Viñas, M Centelles, P Ring, and P Schuck. Erratum: Relativistic mean-field interaction with density-dependent meson-nucleon vertices based on microscopical calculations [phys. rev. c 84, 054309 (2011)]. *Physical Review C*, 93(6):069905, 2016.
- [42] Sha Wang, Hong Fei Zhang, Jian Ming Dong, et al. Neutron star properties in density-dependent relativistic mean field theory with consideration of an isovector scalar meson. *Physical Review C*, 90(5):055801, 2014.
- [43] V. Dexheimer, R. Negreiros, and S. Schramm. Reconciling nuclear and astrophysical constraints. *Phys. Rev. C*, 92:012801, Jul 2015.
- [44] Bharat Kumar, S. K. Patra, and B. K. Agrawal. New relativistic effective interaction for finite nuclei, infinite nuclear matter, and neutron stars. *Phys. Rev. C*, 97:045806, Apr 2018.
- [45] Ankit Kumar, HC Das, and SK Patra. Incompressibility and symmetry energy of a neutron star. *Physical Review C*, 104(5):055804, 2021.
- [46] Fan Li, Bao-Jun Cai, Ying Zhou, Wei-Zhou Jiang, and Lie-Wen Chen. Effects of Isoscalar- and Isovector-scalar Meson Mixing on Neutron Star Structure. *Astrophys. J.*, 929(2):183, 2022.
- [47] Shashi K Dhiman, Raj Kumar, and B. K. Agrawal. Non-rotating and rotating neutron stars in the extended field theoretical model. *Phys. Rev. C*, 76(4):045801, 2007.
- [48] Raj Kumar, B. K. Agrawal, and Shashi K. Dhiman. Effects of ω meson self-coupling on the properties of finite nuclei and neutron stars. *Phys. Rev. C*, 74:034323, Sep 2006.
- [49] N. K. Glendenning. Compact stars: Nuclear physics, particle physics, and general relativity. *Springer-Verlag, New York*, 2000.
- [50] Meng Wang, WJ Huang, Filip G Kondev, Georges Audi, and Sarah Naimi. The ame 2020 atomic mass evaluation (ii). tables, graphs and references. *Chinese Physics C*, 45(3):030003, 2021.
- [51] István Angeli and Krassimira Petrova Marinova. Table of experimental nuclear ground state charge radii: An update. *Atomic Data and Nuclear Data Tables*, 99(1):69–95, 2013.
- [52] Peter Ring and Peter Schuck. *The nuclear many-body problem*. Springer Science & Business Media, 1980.
- [53] S Karatzikos, AV Afanasjev, GA Lalazissis, and P Ring. The fission barriers in actinides and superheavy nuclei in covariant density functional theory. *Physics Letters B*, 689(2-3):72–81, 2010.
- [54] T. Duguet, P. Bonche, P.-H. Heenen, and J. Meyer. Pairing correlations. ii. microscopic analysis of odd-even mass staggering in nuclei. *Phys. Rev. C*, 65:014311, Dec 2001.
- [55] Wei-Chia Chen and Jorge Piekarewicz. Searching for isovector signatures in the neutron-rich oxygen and calcium isotopes. *Physics Letters B*, 748:284–288, 2015.
- [56] C. Mondal, B. K. Agrawal, J. N. De, and S. K. Samaddar. Sensitivity of elements of the symmetry energy of nuclear matter to the properties of neutron-rich systems. *Phys. Rev. C*, 93:044328, Apr 2016.
- [57] B. K. Agrawal, S. Shlomo, and V. Kim Au. Determination of the parameters of a skyrme type effective interaction using the simulated annealing approach. *Phys. Rev. C*, 72:014310, Jul 2005.
- [58] TJ Bürvenich, DG Madland, and P-G Reinhard. Adjustment studies in self-consistent relativistic mean-field models. *Nuclear Physics A*, 744:92–107, 2004.
- [59] Scott Kirkpatrick. Optimization by simulated annealing: Quantitative studies. *Journal of statistical physics*, 34(5):975–986, 1984.
- [60] J Dobaczewski, W Nazarewicz, and PG Reinhard. Error estimates of theoretical models: a guide. *Journal of Physics G: Nuclear and Particle Physics*, 41(7):074001, 2014.
- [61] C Mondal, BK Agrawal, and JN De. Constraining the symmetry energy content of nuclear matter from nuclear masses: A covariance analysis. *Physical Review C*, 92(2):024302, 2015.
- [62] Siegmund Brandt. *Statistical and computational methods in data analysis*. Springer, 1997.
- [63] P.-G. Reinhard and W. Nazarewicz. Information content of a new observable: The case of the nuclear neutron skin. *Phys. Rev. C*, 81:051303, 2010.
- [64] F. J. Fattoyev, C. J. Horowitz, J. Piekarewicz, and Brendan Reed. Gw190814: Impact of a 2.6 solar mass neutron star on the nucleonic equations of state. *Phys. Rev. C*,

- 102:065805, Dec 2020.
- [65] P Klüpfel, P-G Reinhard, TJ Bürvenich, and JA Maruhn. Variations on a theme by skyrme: A systematic study of adjustments of model parameters. *Physical Review C*, 79(3):034310, 2009.
- [66] Bao-An Li and Xiao Han. Constraining the neutron-proton effective mass splitting using empirical constraints on the density dependence of nuclear symmetry energy around normal density. *Physics Letters B*, 727(1-3):276–281, 2013.
- [67] Tong-Gang Yue, Lie-Wen Chen, Zhen Zhang, and Ying Zhou. Constraints on the symmetry energy from pre-ii in the multimessenger era. *Physical Review Research*, 4(2):L022054, 2022.
- [68] G Colo, U Garg, and H Sagawa. Symmetry energy from the nuclear collective motion: constraints from dipole, quadrupole, monopole and spin-dipole resonances. *The European Physical Journal A*, 50(2):1–12, 2014.
- [69] J Piekarewicz. Symmetry energy constraints from giant resonances: A relativistic mean-field theory overview. *The European Physical Journal A*, 50(2):1–18, 2014.
- [70] Wei-Chia Chen and J. Piekarewicz. Building relativistic mean field models for finite nuclei and neutron stars. *Phys. Rev. C*, 90:044305, 2014.
- [71] Noemi Zabari, Sebastian Kubis, and Włodzimierz Wójcik. Influence of the interactions of scalar mesons on the behavior of the symmetry energy. *Phys. Rev. C*, 99:035209, Mar 2019.
- [72] Noemi Zabari, Sebastian Kubis, and Włodzimierz Wójcik. Anomalous quartic term in the expansion of the symmetry energy. *Phys. Rev. C*, 100:015808, Jul 2019.
- [73] Tsuyoshi Miyatsu, Myung-Ki Cheoun, and Koichi Saito. Asymmetric nuclear matter in relativistic mean-field models with isoscalar-and isovector-meson mixing. *The Astrophysical Journal*, 929(1):82, 2022.
- [74] S Kubis and Marek Kutschera. Nuclear matter in relativistic mean field theory with isovector scalar meson. *Physics Letters B*, 399(3-4):191–195, 1997.
- [75] H Thankful Cromartie, Emmanuel Fonseca, Scott M Ransom, Paul B Demorest, Zaven Arzoumanian, Harsha Blumer, Paul R Brook, Megan E DeCesar, Timothy Dolch, Justin A Ellis, et al. Relativistic shapiro delay measurements of an extremely massive millisecond pulsar. *Nature Astronomy*, 4(1):72–76, 2020.
- [76] Emmanuel Fonseca, HT Cromartie, Timothy T Pennucci, Paul S Ray, A Yu Kirichenko, Scott M Ransom, Paul B Demorest, Ingrid H Stairs, Zaven Arzoumanian, Lucas Guillemot, et al. Refined mass and geometric measurements of the high-mass psr j0740+ 6620. *The Astrophysical Journal Letters*, 915(1):L12, 2021.
- [77] Y Sugahara and H Toki. Relativistic mean-field theory for unstable nuclei with non-linear σ and ω terms. *Nucl. Phys. A*, 579(3-4):557–572, 1994.
- [78] Brendan T Reed, Farrukh J Fattoyev, Charles J Horowitz, and Jorge Piekarewicz. Implications of prex-2 on the equation of state of neutron-rich matter. *Physical Review Letters*, 126(17):172503, 2021.
- [79] Tanja Hinderer. Tidal love numbers of neutron stars. *Astrophys. J.*, 677(2):1216, 2008.
- [80] Tanja Hinderer, Benjamin D Lackey, Ryan N Lang, and Jocelyn S Read. Tidal deformability of neutron stars with realistic equations of state and their gravitational wave signatures in binary inspiral. *Phys. Rev. D*, 81(12):123016, 2010.
- [81] Yuxi Li, Houyuan Chen, Dehua Wen, and Jing Zhang. Constraining the nuclear symmetry energy and properties of the neutron star from gw170817 by bayesian analysis. *The European Physical Journal A*, 57(1):1–10, 2021.
- [82] Yuxi Li, Houyuan Chen, Dehua Wen, and Jing Zhang. Constraining the nuclear symmetry energy and properties of the neutron star from gw170817 by bayesian analysis. *The European Physical Journal A*, 57(1):1–10, 2021.
- [83] Benjamin P Abbott, Rich Abbott, T. D. Abbott, Fausto Acernese, Kendall Ackley, Carl Adams, Thomas Adams, Paolo Addesso, R. X. Adhikari, V. B. Adya, et al. Gw170817: observation of gravitational waves from a binary neutron star inspiral. *Phys. Rev. Lett.*, 119(16):161101, 2017.